Chiang Mai J. Sci. 2020; 47(1) : 195-206
http://epg.science.cmu.ac.th/ejournal/
Contributed Paper

Theoretical Study of Sulfur-containing Compounds Adsorption on Transition Metals (V, Ni, Co, Fe) Doped NbS_2 Surface for Hydrodesulfurization Reaction

Suparada Kamchompoo [a], Tanabat Mudchimo [a], Yutthana Wongnongwa [a], Manaschai Kunaseth*[b], and Siriporn Jungsuttiwong*[a]

[a] Department of Chemistry and Center of Excellence for Innovation in Chemistry, Faculty of Science, Ubon Ratchathani University, Ubon Ratchathani 34190, Thailand.

[b] National Nanotechnology Center (NANOTEC), National Science and Technology Development Agency (NSTDA), Klong Luang, Pathum Thani 12120, Thailand.

*Author for correspondence; e-mail: manaschai@nanotec.or.th, siriporn.j@ubu.ac.th

Received: 5 August 2019
Revised: 18 October 2019
Accepted: 20 October 2019

Abstract

The HDS reaction is one of the most important hydrotreating processes in petroleum refineries that use for removal of sulfur (S) compound from the crude oil. In this work, the adsorption of thiophene (C_4H_4S), benzothiophene (C_8H_6S), and hydrogen sulfide (H_2S) on pure and transition metals (V, Ni, Co, Fe) doped niobium sulfide (NbS_2) surface were investigated by density functional theory (DFT) calculations to further investigate the HDS reaction mechanism of S-containing compounds on this surface. The results show that in all case, the H_2S, C_4H_4S and C_8H_6S preferred to adsorb on the metal edge sites (M-edge) of V doped NbS_2 (V/NbS_2) surface with adsorption energies (E_{ads}) of -0.80, -0.79 and -1.38 eV, respectively. It was found that the C_8H_6S shows strongest adsorption energy because it exhibits significantly stronger π-interaction between C_8H_6S and V/NbS_2 surface, compared to others. The understanding gained in the current study might be helpful in the development of active catalysts for the HDS reaction of S-containing compounds in petroleum oil production.

Keywords: hydrodesulfurization, transition metals doped niobium sulfide surface, S-containing compounds, hydrotreating processes

1. Introduction

In the past decade, petroleum oil was a critical source of fossil fuels that are still widely used in transportation and chemical industry, and it is expected to continue to increase the usage rate of fossil fuels continuously.[1] According to a recent article, the natural fossil fuels contain sulfur-containing compounds that are the most abundant contaminated in fuel oil that must be removed during petroleum processing. The sulfur-containing compounds found in fossil fuels include non-heterocycle and heterocycle such as hydrogen sulfide, thiophene and benzothiophene. Furthermore, without the removal of sulfur-containing compounds, when the combustion reaction of sulfur-containing compounds in fuel will release SO_x species (SO_2 and SO_3), which is the main cause

of acid rain to the environment and contribute to global climate change.[2-5] It is also a problem in a cycle of atmospheric gas chemistry leading to the ozone depletion and decreasing air quality. Consequently, governments and organizations around the world have implemented strict environmental regulations to reduce or limit SO_2 emissions and the amount of sulfur contents in the fossil fuels. Although researchers are currently trying to find sustainable alternative fuel sources, fossil fuels are still necessary in the years to come. Therefore, it is necessary to find ways to reduce the level of sulfur-containing compounds in the fuels prior to their use.[6] This requires the refinery process to remove sulfur via the hydrodesulfurization (HDS) reaction. Which in this process works quite well for aliphatic sulfur compounds removal, but is less effective for aromatic thiophene and its derivatives, which are the main sulfur species left in fuel oil.[7,8] Therefore, the study of thiophene and its derivatives adsorption on the surface of catalysts is considered as the first step of sulfur removal process for HDS reactions.

The HDS reaction is one of the most important processes of hydrotreating in petroleum refineries, which will cause S-containing compounds to be removed from crude oil. Here, the S-containing compounds in crude oil react with hydrogen gas (H_2) forming hydrogen sulfide (H_2S) and an S-free hydrocarbon compounds as a clean fuel. [1,2,9-12] The HDS reaction can be described by the following equation.

$$C_mH_nS + xH_2 \rightarrow H_2S + \text{hydrocarbons} \quad (1)$$

The transition-metal sulfide (TMS) catalytic materials are one of the most commonly used for HDS process with high conversion efficiency.[6,13-17] Among the TMS catalytic materials, molybdenum sulfide (MoS_2) have been found as an excellent catalytic materials for HDS process, not only for the high efficiency but also showed the high selectivity for S-containing compound removals. However, the HDS reaction on MoS_2 surface is performed via a catalytic process using high hydrogen pressure and high operating temperature and the HDS process is less effective for aromatic sulfur species such as thiophene, benzothiophene, and dibenzothiophene. [13,18-20] Moreover, The E_{ads} of thiophene and benzothiophene on MoS_2 surface is in range of -0.5 to -0.7 eV, which is less stable adsorption. [21-25] From these results, it needs to improve the new catalysts for the HDS reaction at low hydrogen pressure and low operating temperature.

Recently, H. Pan et al.[26] studied the hydrogen evolution reduction of metal dichalcogenides (MX_2; M = Nb, Ta, and V; X = S, Se, and Te) monolayers using DFT calculations. They found that the MS_2 monolayers show better catalytic performance than the MSe_2 and MTe_2 monolayers for hydrogen production. X. Chen et al.[27] investigated the hydrogen adsorption for origin of hydrogen evolution activity on the monolayers of MS_2 (M = Mo or Nb) in both 1H and 1T phases using DFT calculations. It is found that the 1H-NbS_2, 1T-MoS_2 and 1T-NbS_2 monolayers show strong H adsorption rather another surface. S. Zhao et al.[28] studied the activity of oxygen reduction reaction (ORR) on MX_2 (M = Nb, Ta, Mo, W; X = S, Se, Te) surfaces using DFT calculations. The results show that the NbS_2 and $TaTe_2$ surfaces exhibit the best performance ORR activity. R. Oviedo-Roa et al.[10] studied the relationship between electronic properties and HDS catalytic activity over the different 4d-TMS surfaces (NbS, NbS_2, MoS_2, TcS_2, RuS_2, Rh_2S_3, PdS, and PdS_2) using the periodic plane-wave pseudopotential technique as implemented in the CASTEP software package. They found that 4d-TMS surfaces are high activity for HDS reaction. Y. Aray et al.[17] studied the M-edge sites of pure and V, Fe, Co, and Ni doped NbS_2 surface by using DFT calculations. The results show that Ni, Co, and V promoters were stabilized on NbS_2 surface at the HDS conditions. Based on theoretical and experimental evidences, NbS_2 supported catalyst is potential candidate for catalytic HDS. However, the adsorption of the S-containing compounds for the HDS reaction on TMS doped NbS_2 catalysts

has not yet been investigated.

Despite many contributions from experimental and theoretical studies on the HDS reaction of S-containing compounds on TMS catalysts, the adsorption and elementary reaction steps of S-containing compounds for the HDS reaction on NbS_2-based catalysts has not yet been elucidated. In this work, we investigated the adsorption of C_4H_4S, C_8H_6S, and H_2S on the V, Fe, Co, and Ni doped NbS_2 surface by using DFT calculations. The understanding gained in the current study might be helpful in the development of active catalysts for the HDS reaction of S-containing compounds in petroleum oil production.

2. COMPUTATIONAL DETAILS

2.1. DFT Calculations

All calculations were performed by using the plane-wave based periodic DFT method implemented in the Vienna ab initio simulation package (VASP), where the ionic cores are described by the projector augmented wave (PAW) method. The exchange and correlation energies are computed using the Perdew-Burke-Ernzerhof (PBE) functional along with the dispersion correction to account for van der Waals interaction (PBE-D3). To have accurate energies, a plane-wave cutoff energy of 400 eV, the Gaussian electron smearing method with σ = 0.10 eV were used. The Brillouin zone integrations were performed using the Monkhorst-Pack grids of 15 × 15 × 15 and 3 × 3 × 1 for the bulk and surface calculations, respectively. An isolated gas molecules was placed in a 15 Å x 15 Å x 15 Å box. Geometry optimization was performed until the forces acting on each atom were smaller than 0.05 eV/Å with the electronic self-consistent field iteration threshold of 10^{-6} eV.

2.2. Model

According to previous work,[17] the NbS_2 bulk has a similar structure or almost identical to the MoS_2 bulk. The NbS_2 bulk has a hexagonal crystal structure and belonging to the $P6_3/mmc$ space group.[10,29,30] In NbS_2 bulk, locally six S atoms are coordinated to one niobium atom to form a trigonal prismatic arrangement. The NbS_2 (100) plane was cleaved from NbS_2 bulk. Then, the cleaved plane increased to four layers slab and 4x1 supercell as shown in **Figure 1.** A vacuum thickness of 18 Å was employed to separate each slab from interactions between slabs. In the NbS_2 (100) surface, the first two layers are allowed to relax, whereas the two bottom layers are fixed in their bulk position. Moreover, we have studied the V, Fe, Co, and Ni doped at the M-edge sites of the NbS_2 surfaces (V/NbS_2, Fe/NbS_2, Co/NbS_2, and Ni/NbS_2 surfaces) as shown in **Figure 2**. The four Nb atoms at the M-edge sites of pure NbS_2 surface can be substituted by the four atoms of V, Fe, Co, and Ni to create the V, Fe, Co, and Ni doped NbS_2 surface.[17]

2.3 Analysis of Substitution Energy and Adsorption Energy

The substitution energies (E_{sub}) of promoted transition metal (TM) atoms on NbS_2 surface were calculated according to the following equation (2):

$$E_{sub} = (E_{TMS/NbS_2} - E_{NbS_2} - (4E_{TM} - 4E_{Nb}))/4 \quad (2)$$

Where E_{TMS/NbS_2} is the total energy of the TMS doped NbS_2 surface, E_{NbS_2} is the total energy of the bare NbS_2 surface, E_{TM} is the total energy of the TM atom, and E_{Nb} is the total energy of the Nb atom. The stability of the V, Fe, Co, and Ni doped NbS_2 surface were considered by E_{sub} value. The less positive E_{sub} value refers to high stability of the promoted TMS on NbS_2 surface.

The adsorption energies (E_{ads}) of S-containing compounds on the NbS_2-based surface were calculated according to the following equation (3):

$$E_{ads} = E_{molecule/surface} - E_{surface} - E_{molecule} \quad (3)$$

Where $E_{molecule/surface}$ is the total energy of the S-containing compound adsorption on NbS_2-based surface; $E_{surface}$ is the total energy of the NbS_2-based surface; and $E_{molecule}$ is the total

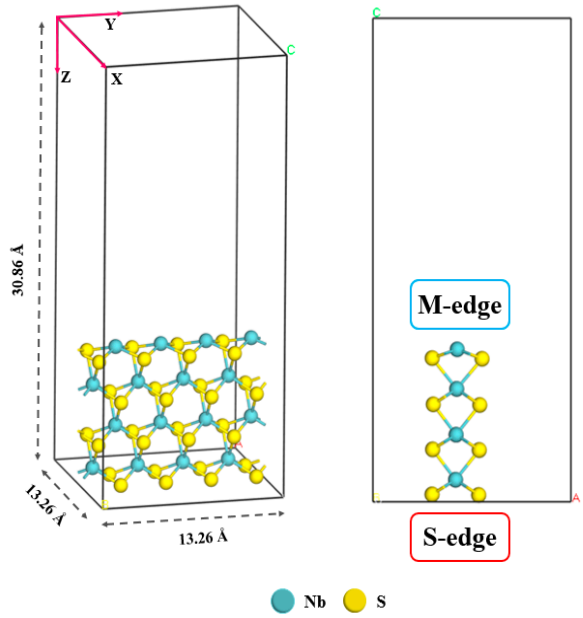

Figure 1. The monolayer model of NbS_2 (100) surface showing the M-edge and the S-edge sites.

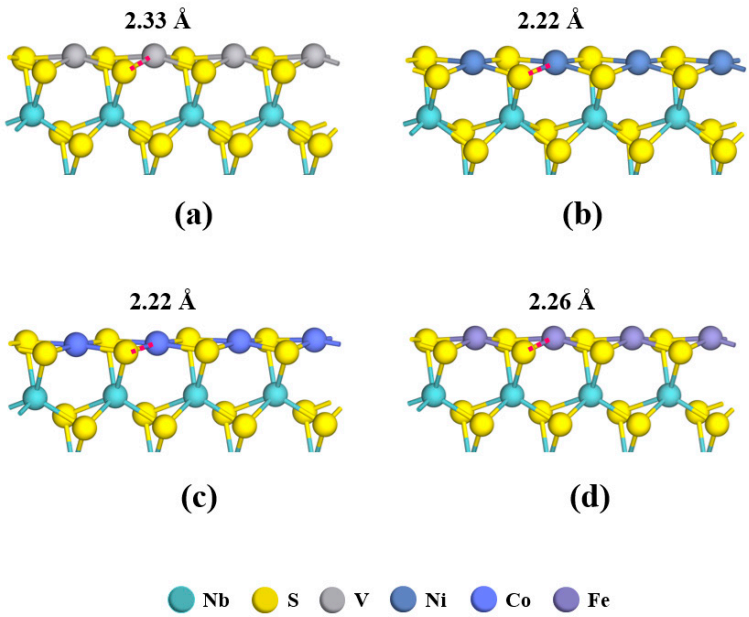

Figure 2. Supercell configurations of (a) V/NbS_2, (b) Ni/NbS_2, (c) Co/NbS_2, and (d) Fe/NbS_2 surfaces.

energy of S-containing compound molecule. The negative E_{ads} value represents the energetically favorable adsorption between the S-containing compounds and the NbS_2-based surface.

In addition, the difference bader charges (Q) between the gas molecule (S-containing compounds) and NbS_2-based surface were calculated according to the following equation (4).

$$Q = Q_f - Q_b \quad (4)$$

Where Q_f is the amounts of carried charge of the gas molecules after adsorption on surface; and Q_b is the amounts of carried charge of the gas molecules before adsorption on surface. Which is calculated by electron population analysis. The positive Q value represents the electrons transfer form gas molecule (S-containing compounds) to surface.

3. RESULT AND DISCUSSIONS

3.1 The V, Ni, Co, and Fe Doped NbS_2 Surface

In this section, we considered the V, Fe, Co, and Ni doped NbS_2 surface for the adsorption of S-containing compounds. The optimized geometry of the pure and V, Fe, Co, and Ni doped NbS_2 surface are displayed in **Figure 1 and 2.** The electronic property parameters of the promoted V, Fe, Co, and Ni on NbS_2 surface are shown in **Table 1**. The E_{sub} value of various surfaces is as the following order: V/NbS_2 (2.21 eV) < Ni/NbS_2 (2.80 eV) < Co/NbS_2 (2.86 eV) < Fe/NbS_2 (3.33 eV), which correspond to previous work. [17] The results show that the E_{sub} value of V/NbS_2 surface is the lowest E_{sub} value. The less positive E_{sub} refer to higher stability of promoted metal on NbS_2 surface. In addition, the average bond length between TM atoms and S atoms in the first layer (d_{TM-S}) of V/NbS_2 surface (2.33 Å) close to the d_{TM-S} of pure NbS_2 surface (2.43 Å). From these results, it indicated that the V/NbS_2 surface is more stable than the Ni/NbS_2, Co/NbS_2, and Fe/NbS_2 surfaces. To understand the electronic properties of the TMS doped NbS_2 (TMS/NbS_2) surfaces, we calculated the average bader charge of Nb, V, Fe, Co, and Ni atoms in the first layer of NbS_2-based surfaces (Q_{TM}). The results show that the Q_{TM} of V/NbS_2 surface is 1.28 $\bar{e}$, which is the most positive value. It indicated that the V/NbS_2 surface is the most active surface for S-containing compounds.

Table 1. The substitution energies (E_{sub}), average bond length between TM atoms and S atoms in the first layer (d_{TM-S}), and average bader charge of TM atoms in the first layer (Q_{TM}) of the pure and V, Fe, Co, and Ni doped NbS_2 surfaces.

Surfaces	E_{sub} (eV)	d_{TM-S} (Å)	Q_{TM} ($\bar{e}$)
pure NbS_2	0.00	2.43	1.17
V/NbS_2	2.21	2.33	1.28
Ni/NbS_2	2.80	2.22	0.55
Co/NbS_2	2.86	2.22	0.28
Fe/NbS_2	3.33	2.26	0.99

3.2 The S-containing Compounds Adsorption on Various Surfaces

In this section, the adsorption of C_4H_4S, C_8H_6S, and H_2S on the pure and V, Fe, Co, and Ni doped NbS_2 surfaces were investigated by DFT calculations. It was classified into 3 parts: (I) C_4H_4S, (II) C_8H_6S, and (III) H_2S adsorption on the pure and V, Fe, Co, and Ni doped NbS_2 surfaces. For each adsorbate, only adsorption sites and structures with the largest adsorption energies are included, although all possible adsorption sites have been evaluated.

3.2.1 The H_2S adsorption on various surfaces

In the final part, the adsorption of H_2S on pure NbS_2 and promoted V, Fe, Co, and Ni on NbS_2 surfaces were investigated. The adsorption structures, energies, difference bader charges, and bond lengths of the H_2S adsorption on various surfaces are presented in **Figure 3**. For the H_2S adsorption on pure NbS_2 surface, the S atom of H_2S molecule binds to M-edge site of pure NbS_2 surface with E_{ads} of -0.81 eV (**Figure 3a)**. Similarly to NbS_2 surface, the H_2S adsorbed on the M-edge site of TMS/NbS_2 surfaces with bonding between the S atom of H_2S molecule and TM atom of surfaces as shown in **Figure 3b-e**. The H_2S adsorbed on Co, Ni, and Fe doped NbS_2 surfaces with E_{ads} of -1.29, -1.26, and -1.15 eV, respectively, which are stronger than that on bare NbS_2 surface (-0.81 eV). On the other hand, the H_2S adsorbed on V/NbS_2 surface with E_{ads} = -0.80 eV (**Figure 3b**), which is weaker than that on other surfaces. In order to confirm these results, the difference bader charges of H_2S molecule between before and after adsorption on various surfaces (ΔQ_H) are considered. The results show that the ΔQ_H value of the H_2S adsorption on V/NbS_2 surface (0.06 e) is lower than that on Co, Ni, and Fe doped NbS_2 surfaces. It indicated that the electrons transfer of H_2S molecule to V/NbS_2 surface is lower than that to the Co, Ni, and Fe doped NbS_2 surfaces, which results in the E_{ads} value of the H_2S on V/NbS_2 surface lower than that on other surfaces.

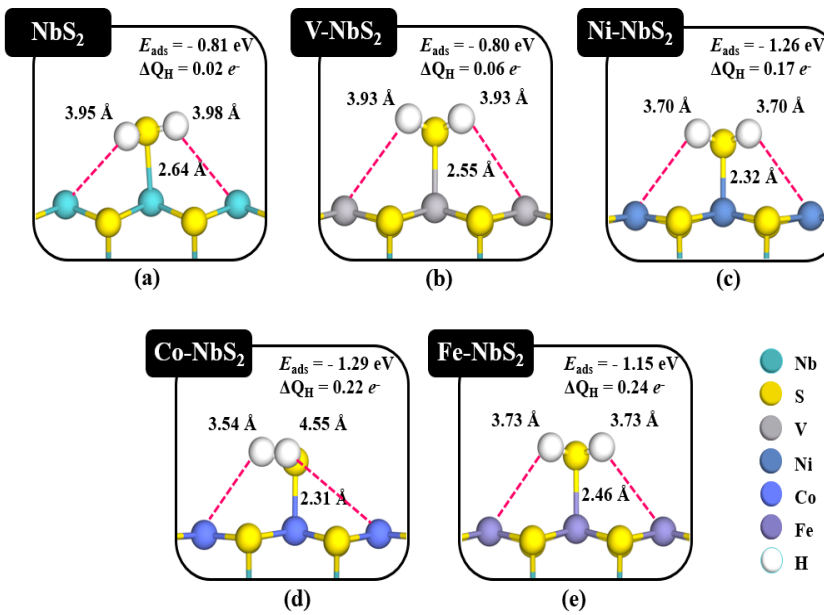

Figure 3. The most stable adsorption structures of H_2S molecule on the metal edge site of the pure and V, Fe, Co, and Ni doped NbS_2 surfaces.

3.2.2 The C_4H_4S adsorption on various surfaces

In the first part, the C_4H_4S adsorption on pure NbS_2 and promoted V, Fe, Co, and Ni on NbS_2 surfaces are investigated. The adsorption structures, energies, difference bader charges, and bond lengths of the C_4H_4S adsorption on various surfaces are shown in **Figure 4**. For the C_4H_4S adsorption on pure NbS_2 surface, the S atom and two C atoms of the C_4H_4S molecule bind to Nb atom of surface with E_{ads} of -0.70 eV (**Figure 4a**). For the C_4H_4S adsorption on TMS/NbS_2 surfaces as shown in **Figure 4b-d**, the C_4H_4S molecule adsorbed on V, Ni, Co doped NbS_2 surfaces with E_{ads} of -0.79, -0.74, and -0.74 eV, respectively, which are stronger than that on pure NbS_2 surface (-0.70 eV). On the other hand, the C_4H_4S adsorption on Fe doped NbS_2 surface (-0.63 eV) as shown in **Figure 4e** is weaker than that on pure NbS_2 surface (-0.70 eV). The C_4H_4S adsorbed on TMS/NbS_2 surfaces with only S atom of C_4H_4S, which is directly binds to the TM of surfaces. The E_{ads} of C_4H_4S on the V, Ni, and Co doped NbS_2 surfaces are in the range between -0.74 to -0.79 eV, which is stronger than previous works as show in **Table 2**.[6,21-25] In order to confirm these results, the difference bader charges of C_4H_4S molecule between before and after adsorption on various surfaces (ΔQ_T) are considered. The results show that the ΔQ_T value of the C_4H_4S adsorption on V/NbS_2 surface (0.21 e) is higher than others. It indicated that the electrons transfer of C_4H_4S molecule to V/NbS_2 surface is higher than others, which results in the E_{ads} value of the C_4H_4S on V/NbS_2 surface rather than that on other surfaces.

3.2.3 The C_8H_6S adsorption on various surfaces

In this section, we present a detailed investigation of structures and energies for C_8H_6S adsorption on pure NbS_2 and promoted with V, Ni, Co, and Fe on NbS_2 surfaces. The adsorption structures, energies, difference bader charges, and bond lengths of the C_8H_6S adsorption on various surfaces are shown in **Figure 5.** For the C_8H_6S adsorption on

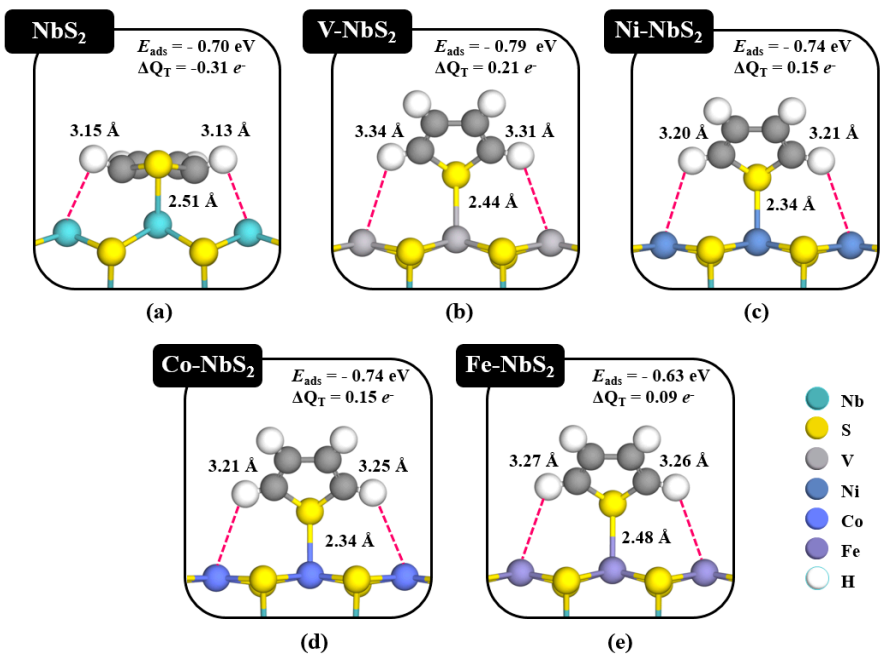

Figure 4. The most stable adsorption structures of C_4H_4S molecule on the metal edge site of the pure and V, Fe, Co, and Ni doped NbS_2 surfaces.

Table 2. The adsorption energy (E_{ads}) of C_4H_4S, C_8H_6S, and H_2S adsorbed on TMs surface.

TMs surface	E_{ads} (eV)		
	C_4H_4S	C_8H_6S	H_2S
MoS_2 [a]	-0.59	-	-
Ni/MoS_2 [a]	-0.60	-0.69	-0.80
Co/MoS_2 [a]	-0.57	-	-
NbS_2 [b]	-0.70	-0.88	-0.81
V/NbS_2 [b]	-0.79	-1.38	-0.80
Ni/NbS_2 [b]	-0.74	-1.21	-1.26
Co/NbS_2 [b]	-0.74	-1.12	-1.29
Fe/NbS_2 [b]	-0.63	-0.11	-1.15

[a] Atom labels represent the calculation from previous research.
[b] Atom labels represent the calculation from our research.

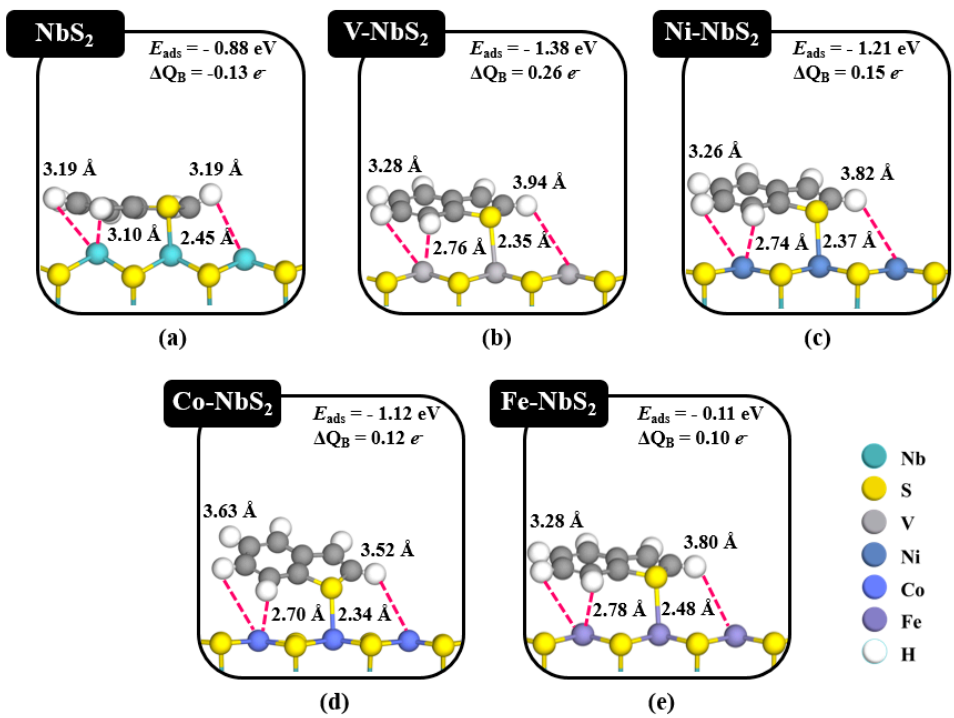

Figure 5. The most stable adsorption structures of C_8H_6S molecule on the metal edge site of the pure and V, Fe, Co, and Ni doped NbS_2 surfaces.

pure NbS_2 surface, the C_8H_6S molecule interacts with pure NbS_2 surface by pi-interaction, which pi-bond of C_8H_6S ring bond to Nb atom of surface with E_{ads} of -0.88 eV (**Figure 5a**). For the C_8H_6S adsorption on TMS/NbS_2 surfaces as shown in **Figure 5b-d**, the C_8H_6S molecule adsorbed at the M-edge site of V, Ni, Co doped NbS_2 surfaces with E_{ads} of -1.38, -1.21, and -1.12 eV, respectively, which are higher than that of pure NbS_2 surface (-0.88 eV). On the other hand, the E_{ads} of C_8H_6S molecule weak adsorbed on Fe/NbS_2 surface with E_{ads} = -0.11 eV (**Figure 5e**). Moreover, the C_8H_6S adsorbed on TMS/NbS_2 surfaces by π-interaction with π-bond of C_8H_6S ring bond to TMS on surface, which is directly binds to the TM atom of surfaces. The E_{ads} of C_8H_6S on the M-edge site of promoted V, Ni, and Co on NbS_2 surfaces are in the range between -0.88 to -1.38 eV, which is stronger than previous work as show in table 2.[24] To confirm these results, the difference bader charges of C_8H_6S molecule between before and after adsorption on various surfaces (ΔQ_B) are considered. The results show that the ΔQ_B value of the C_8H_6S adsorption on V/NbS_2 surface (0.26 *e*) is higher than others. It indicated that the electrons transfer of C_8H_6S molecule to V/NbS_2 surface is higher than others, which results in the E_{ads} value of the C_8H_6S on V/NbS_2 surface rather than that on other surfaces.

To provide a further understanding of electronic binding properties of V/NbS_2 surface, the partial density of states (PDOS) analysis of the C_4H_4S, C_8H_6S, and H_2S adsorption on V/NbS_2 surface were investigated as shown in **Figure 6**. The figure shows that the S 3p orbital of S-containing compounds spans a sharp energy range and overlaps the 3d orbital of V atom on the surface at the lower region from the Fermi level (E_F). The S 3p orbital density peaks of C_8H_6S appear in the same regions as the 3d orbital of V atom on surface, indicating that V atom on surface interacts strongly with the S 3p orbital of C_8H_6S. This interaction is weaker for C_4H_4S and H_2S adsorption on V/NbS_2 surface, in which only sharp peaks and small peaks are presented in the same region as the 3d orbital of V atom on the surface. From these results, the PDOS analysis can confirm the strong interaction between C_8H_6S molecule and V-NbS_2 surface, which correspond to the high E_{ads} and ΔQ_B values in section 3.2.3. In addition, it can confirm the weaker interaction between C_4H_4S and H_2S on V-NbS_2 surface, which correspond to the low E_{ads} and ΔQ_H, ΔQ_T values in section 3.2.1 and 3.2.2, respectively.

Moreover, the charge density differences of the C_4H_4S, C_8H_6S, and H_2S on V/NbS_2 surface are illustrated in **Figure 7**, where the charge accumulation and charge depletion are represented by yellow and blue regions, respectively. Our results show that the charge accumulation and charge depletion of the H_2S, C_4H_4S and C_8H_6S adsorption on V/NbS_2 surface are clearly observed, especially C_8H_6S adsorption on the V/NbS_2 surface. From Figure 7a and 7c, H_2S molecule bind to the V/NbS_2 surface via their heteroatom and C_4H_4S molecule bind to the V/NbS_2 surface via π-interaction of C_4H_4S ring. While C_8H_6S molecule bind to the V/NbS_2 surface via π-interaction by five- membered ring and benzene rings of C_8H_6S molecule as show in figure 7b. Therefore, the C_8H_6S adsorption on V/NbS_2 surface indicated that the strong interaction than H_2S and C_4H_4S molecule. These results correspond to the ΔQ_B values, which show a large number of electrons transfer from C_8H_6S molecules to the V/NbS_2 surface (0.26 *e*) and small number of electrons transfer from H_2S molecule to the V/NbS_2 surface (0.06 *e*).

From our results, it indicated that the V/NbS_2 surface is the most active surface for S-containing compounds. The H_2S, C_4H_4S and C_8H_6S adsorption on V/NbS_2 surface are strong adsorption. In addition, it was found that from charge density difference of C_8H_6S shows that C_8H_6S molecule adsorption on V/NbS_2 surface using bonding between S atom and C atom of C_8H_6S molecule bind to V atom of surface. Therefore, the C_8H_6S molecule adsorption on

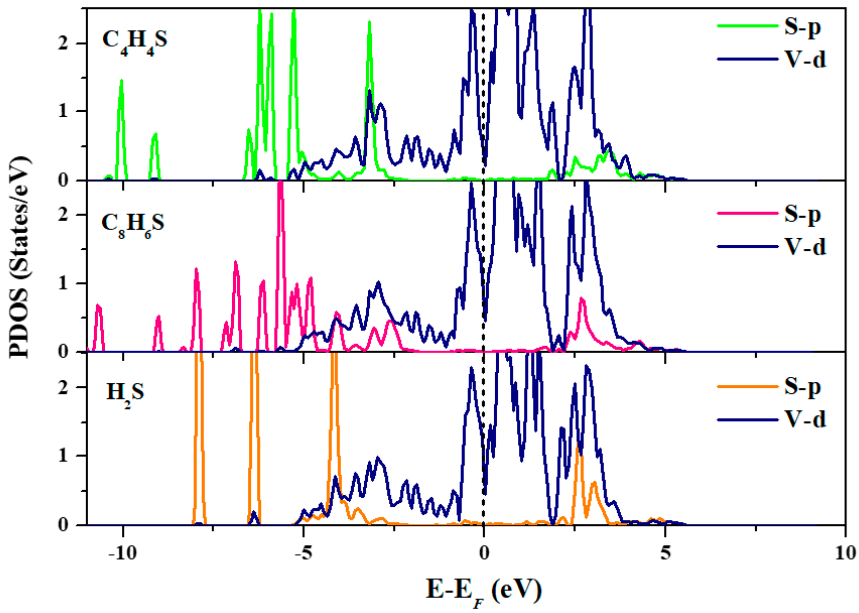

Figure 6. The PDOS analysis of the C_4H_4S, C_8H_6S, and H_2S adsorption on V-NbS_2 surface.

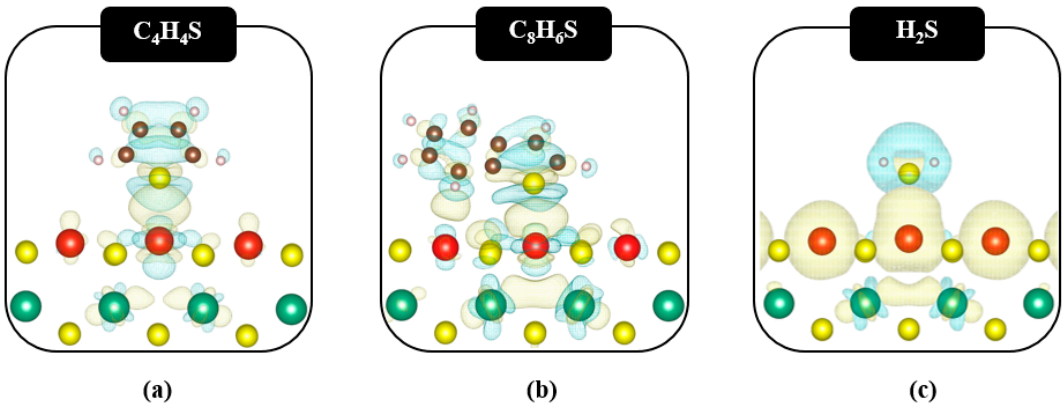

Figure 7. Charge density differences of the C_4H_4S, C_8H_6S, and H_2S adsorption on the V-NbS_2 surface with isovalue of ± 0.004 e/Å^3. Charge accumulation and depletion are represented by yellow and blue regions, respectively.

V/NbS_2 surface is stronger than H_2S and C_4H_4S molecule. These results are confirmed using the E_{ads}, ΔQ and PDOS of the C_4H_4S, C_8H_6S, and H_2S adsorption on the V-NbS_2 surface. The results show that the V/NbS_2 surface should be a good catalyst for the HDS reaction of H_2S, C_4H_4S and C_8H_6S. Finally, the knowledge of the C_4H_4S, C_8H_6S, and H_2S adsorption on the V, Ni, Co, and Fe doped NbS_2 catalysts is essential for the development of the NbS_2-based catalysts for the HDS reaction of S-containing compounds.

4. Conclusions

In this work, the H_2S, C_4H_4S and C_8H_6S adsorption on pure and V, Ni, Co, Fe doped NbS_2 surfaces were investigated by DFT calculations to further investigate the HDS reaction mechanism of S-containing compounds on these surfaces. The results show that in all case, the H_2S, C_4H_4S and C_8H_6S preferred to adsorb on the metal edge sites (M-edge) of V doped NbS_2 (V/NbS_2) surface. Especially, for the case of the C_8H_6S adsorbed on the V/NbS_2 surface with E_{ads} of -1.38 eV, which are more stable than that on other surfaces. The ΔQ_B values for the V/NbS_2 surface are 0.26 e^-, which are higher than others. It indicated that the electron transfer from the C_8H_6S molecules to the V/NbS_2 surface are higher than that to other surfaces. On the other hand, the H_2S adsorbed on the Co, Ni, and Fe doped NbS_2 surfaces with E_{ads} of -1.29, -1.26, and -1.15 eV, respectively, which are more stable than that on the V/NbS_2 surface (-0.80 eV). The ΔQ_H values for the V/NbS_2 surface (0.06 e) is lower than others. In addition, it was found that from charge density difference of C_8H_6S shows that C_8H_6S molecule adsorption on V/NbS_2 surface using bonding between S atom and C atom of C_8H_6S molecule bind to V atom of surface. Therefore, the C_8H_6S molecule adsorption on V/NbS_2 surface is stronger than H_2S and C_4H_4S molecule. Moreover, the PDOS analysis and difference bader charge of the C_4H_4S, C_8H_6S, and H_2S adsorption on V/NbS_2 surface are considered, which can confirm the strong interaction of the C_8H_6S adsorption on V/NbS_2 surface and the weak interaction of the H_2S and C_4H_4S adsorption on V/NbS_2 surface. From these results, it indicated that the V/NbS_2 surface could be a potential catalyst for the HDS reaction of S-containing compounds. The understanding gained in the current study might be helpful in the development of active catalysts for the HDS reaction of S-containing compounds in petroleum oil production.

Acknowledgments

The authors are grateful to department of chemistry at Ubon Ratchathani University and the National Nanotechnology Center (NANOTEC) for providing access to their computing resources. S.K. thanks the Thailand Graduate Institute of Science and Technology (TGIST) for financial support.

References

[1] Liu P., Rodriguez J.A., Asakura T., Gomes J. and Nakamura K., *J. Phys. Chem. B*, 2005; **109**: 4575-4583. DOI 10.1021/jp044301x.

[2] Xiao J., Li Z., Liu B., Xia Q. and Yu M., *Energy Fuels*, 2008; **22**: 3858-3863. DOI 10.1021/ef800437e.

[3] Šarić M., Rossmeisl J. and Moses P.G., *Phys. Chem. Chem. Phys.*, 2017; **19**: 2017-2024. DOI 10.1039/C6CP06881B.

[4] Šarić M., Rossmeisl J. and Moses P.G., *J. Catal.*, 2018; **358**: 131-140. DOI 10.1016/j.jcat.2017.12.001.

[5] Han Y., Zhang Y., Xu C. and Hsu C.S., *Fuel*, 2018; **221**: 144-158. DOI 10.1016/j.fuel.2018.02.110.

[6] Huang Y., Liu H., Chen X., Zhou D., Wang C., Du J., Zhou T. and Wang S., *J. Phys. Chem. C*, 2016; **120**: 12012-12021. DOI 10.1021/acs.jpcc.6b02769.

[7] Hernández-Maldonado A.J. and Yang R.T., *Catal. Rev.*, 2004; **46**: 111-150. DOI 10.1081/CR-200032697.

[8] Rui J., Liu F., Wang R., Lu Y. and Yang X., *Molecules*, 2017; **22**: 305. DOI 10.3390/molecules22020305.

[9] Mittendorfer F. and Hafner J., *J. Catal.*, 2003; **214**: 234-241. DOI 10.1016/S0021-9517(02)00149-5.

[10] Oviedo-Roa R., Martínez-Magadán J.-M. and Illas F., *J. Phys. Chem. B*, 2006; **110**: 7951-7966.

DOI 10.1021/jp052299j.

[11] Dzade N.Y. and de Leeuw N.H., *J. Phys. Chem. C*, 2018; **122**: 359-370. DOI 10.1021/acs.jpcc.7b08711.

[12] Jaf Z.N., Altarawneh M., Miran H.A., Jiang Z.-T. and Dlugogorski B.Z., *Mol. Catal.*, 2018; **459**: 21-30. DOI 10.1016/j.mcat.2018.07.008.

[13] Zhu H., Guo W., Li M., Zhao L., Li S., Li Y., Lu X. and Shan H., *ACS Catal.*, 2011; **1**: 1498-1510. DOI 10.1021/cs2002548.

[14] Zheng P., Duan A., Chi K., Zhao L., Zhang C., Xu C., Zhao Z., Song W., Wang X. and Fan J., *Chem. Eng. Sci.*, 2017; **164**: 292-306. DOI 10.1016/j.ces.2017.02.037.

[15] Li G., Zhu H., Zhao L., Guo W., Ma H., Yu Y., Lu X. and Liu Y., *J. Phys. Chem. C*, 2016; **120**: 23009-23023. DOI 10.1021/acs.jpcc.6b07103.

[16] Jin Q., Chen B., Ren Z., Liang X., Liu N. and Mei D., *Catal. Today*, 2018; **312**: 158-167. DOI 10.1016/j.cattod.2018.02.013.

[17] Aray Y., Zambrano D., Cornejo M.H., Ludeña E.V., Iza P., Vidal A.B., Coll D. S., Jímenez D. M., Henriquez F. and Paredes C., *J. Phys. Chem. C*, 2014; **118**: 27823-27832. DOI 10.1021/jp5059269.

[18] Li B., Guo W., Yuan S., Hu J., Wang J. and Jiao H., *J. Catal.*, 2008; **253**: 212-220. DOI 10.1016/j.jcat.2007.10.006.

[19] Yang R.T., Hernández-Maldonado A.J. and Yang F.H., *Science*, 2003; **301**: 79-81. DOI 10.1126/science.1085088.

[20] Bianchini C. and Meli A., *Acc. Chem. Res.*, 1998; **31**: 109-116. DOI 10.1021/ar970029g.

[21] Moses P.G., Hinnemann B., Topsøe H. and Nørskov J.K., *J. Catal.*, 2007; **248**: 188-203. DOI 10.1016/j.jcat.2007.02.028.

[22] Li S., Liu Y., Feng X., Chen X. and Yang C., *Mol. Catal.*, 2019; **463**: 45-53. DOI 10.1016/j.mcat.2018.11.018.

[23] Humbert S., Izzet G. and Raybaud P., *J. Catal.*, 2016; **333**: 78-93. DOI 10.1016/j.jcat.2015.10.016.

[24] Rangarajan S. and Mavrikakis M., *AIChE J.*, 2015; **61**: 4036-4050. DOI 10.1002/aic.15025.

[25] Moses P.G., Hinnemann B., Topsøe H. and Nørskov J.K., *J. Catal.*, 2009; **268**: 201-208. DOI 10.1016/j.jcat.2009.09.016.

[26] Pan H., *Sci. Rep.*, 2014; **4**: 5348. DOI 10.1038/srep05348.

[27] Chen X., Gu Y., Tao G., Pei Y., Wang G. and Cui N., *J. Mater. Chem. A*, 2015; **3**: 18898-18905. DOI 10.1039/C5TA02817E.

[28] Zhao S., Wang K., Zou X., Gan L., Du H., Xu C., Kang F., Duan W. and Li J., *Nano Res.*, 2019; **12**: 925-930. DOI 10.1007/s12274-019-2326-7.

[29] Aray Y. and Rodríguez J., *ChemPhysChem*, 2001; **2**: 599-604. https://doi.org/10.1002/1439-7641(20011015)2:10<599::AID-CPHC599>3.0.CO;2-G

[30] Heil C., Schlipf M. and Giustino F., *Phys. Rev. B*, 2018; **98**: 075120. DOI 10.1103/PhysRevB.98.075120.